

Path-LLM: A Shortest-Path-based LLM Learning for Unified Graph Representation

Wenbo Shang
Hong Kong Baptist University
Hong Kong, China
cswbshang@comp.hkbu.edu.hk

Xuliang Zhu
Antai College of Economics and
Management, Shanghai Jiao Tong
University
Shanghai, China
zhu.xl@sjtu.edu.cn

Xin Huang
Hong Kong Baptist University
Hong Kong, China
xinhuang@comp.hkbu.edu.hk

ABSTRACT

Unified graph representation learning aims to produce node embeddings, which can be applied to multiple downstream applications. However, existing studies based on graph neural networks and language models either suffer from the limitations of numerous training needed toward specific downstream predictions or have shallow semantic features. In this work, we propose a novel Path-LLM model to learn unified graph representation, which leverages a powerful large language model (LLM) to incorporate our proposed path features. Our Path-LLM framework consists of several well-designed techniques. First, we develop a new mechanism of long-to-short shortest path (L2SP) selection, which covers essential connections between different dense groups. An in-depth comparison of different path selection plans is offered to illustrate the strength of our designed L2SP. Then, we design path textualization to obtain L2SP-based training texts. Next, we feed the texts into a self-supervised LLM training process to learn embeddings. Extensive experiments on benchmarks validate the superiority of Path-LLM against the state-of-the-art WalkLM method on two classical graph learning tasks (node classification and link prediction) and one NP-hard graph query processing task (keyword search), meanwhile saving more than 90% of training paths.

1 INTRODUCTION

Graphs play a crucial role in various real-world application scenarios, including academic networks, biomedical graphs, social networks, financial networks, and so on [4, 60, 74]. These graph data associated with textual information, such as the attributes of nodes and edges, representing complex and diverse semantics, are commonly known as text-attributed graphs (TAGs). A wide range of graph representation learning models has been proposed, including successful graph neural networks (GNNs) [19, 26, 36, 68]. However, these models often require sufficient training toward specific downstream predictions [66, 86] and focus more on processing graph structure.

For obtaining graph representation with richer semantics, WalkLM [66] has been recently proposed to integrate *LMs* and *random walks* to derive unified graph embeddings for multiple graph learning tasks, e.g., node classification and link prediction. WalkLM has achieved state-of-the-art in unified graph representation learning but still suffers from the following three limitations. 1) The sampled random walks can hardly cover the bridge edges between different dense groups, as the path of random walk has a high probability of falling within one dense subgraph; 2) random walks can easily involve noisy nodes to damage the embedding quality. Meanwhile,

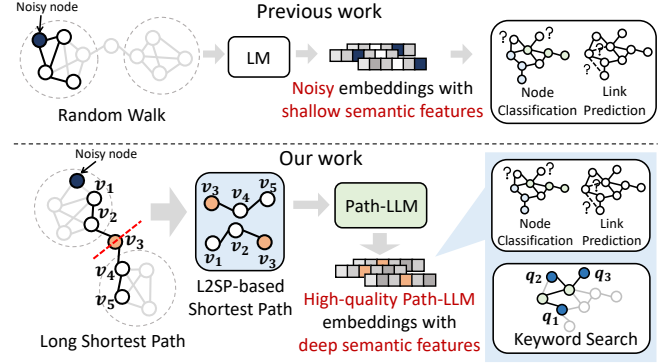


Figure 1: A comparison of WalkLM [66] and our work.

the node texts of irregular paths cannot match the linguistic rules, bringing more difficulty for learning models, and 3) relatively small LMs, such as BERT [13] and DeBERTa [23], generally have weaker performance than the recent LLMs [64].

To tackle the above limitations, we propose a novel graph representation learning model of Path-LLM, as shown in Figure 1. Our developed Path-LLM utilizes *powerful large language models* (LLMs) and *well-designed shortest-path-based graph features* to learn unified graph embeddings for several downstream tasks, including node classification, link prediction, and one typical NP-hard graph analytics task of keyword search [39, 69]. Path-LLM enjoys two major advantages based on *LLMs* and *shortest paths*. First, the advent of LLMs, exemplified by GPT [15, 53], Llama [67], has revolutionized the field of language modeling. LLMs possess billions of parameters and have been trained on extensive corpora, enabling them to exhibit powerful semantic representation capabilities and strong generalization abilities [55, 80, 87]. Second, the shortest path is the closest path between two nodes, which can avoid unnecessary detours through noisy nodes and cycles, in contrast to random walks. The shortest paths usually indicate regular paths to follow in a complex graph, indicating good-quality learning features for LLMs.

It is challenging to achieve a diverse and high-quality set of shortest paths. To tackle it, we construct a new path extraction mechanism to select training features, called the long-to-short shortest paths. It first samples a few long shortest paths to capture cross-group connections and then cuts them into short paths for effective learning. In addition, we design a path textualization function to transform L2SP-based structural information into L2SP-based texts for Path-LLM learning. To embed graph structures into the semantic space, we feed L2SP-based texts into Path-LLM for a self-supervised

pre-training process. As Path-LLM learns the order of tokens in the L2SP-based text, it also learns the order of nodes within the L2SP, thereby learning graph structures. Finally, we derive an integrated embedding for all nodes from the frozen Path-LLM, which is effective for several downstream tasks. To summarize, we make the following contributions:

- We develop a novel Path-LLM model to generate a unified graph embedding. In Path-LLM, we first propose the long-to-short shortest paths (L2SP) and path textual function to construct L2SP-based texts for LLM. We then feed L2SP-based texts into Path-LLM for self-supervised pre-training process and extract Path-LLM embeddings for downstream tasks. (Section 3).
- We conduct a comprehensive analysis by comparing our L2SP method against different path selections to show the advantages and suitability of short paths and L2SP selection in Path-LLM learning (Section 4).
- To illustrate the usefulness of our learned embedding results, we revisit a useful but challenging graph task of keyword search [78], which finds a subgraph covering all keywords with tight closeness of topology structure and node semantics. We develop a method of weighted TAG construction based on the Path-LLM embedding vectors and introduce approximate solutions (Section 5).
- We conduct extensive experiments to validate the effectiveness of Path-LLM outperforming the state-of-the-art WalkLM method on four real-world benchmarks. Our Path-LLM model only uses 9% of WalkLM's training paths on average. We also conduct a case study of keyword search on PubMed and embedding visualization to show the usefulness of our Path-LLM model (Section 6).

We give preliminaries and the problem statement in Section 2. We review related work in Section 7 and conclude the paper in Section 8. Additional analytics material and experiments are reported in APPENDIX.

2 PRELIMINARY

In this section, we introduce the large language models, notations, and the objective of our Path-LLM model.

2.1 Large Language Models

For the pre-training process, LLMs mainly use Causal Language Modeling (CLM) training techniques, which is trained to predict the next token x_i in a sequence $x = \{x_1, x_2, \dots, x_q\}$ based on prefix tokens $x_{<i} = \{x_1, x_2, \dots, x_{i-1}\}$. CLM is commonly used to train LLMs like GPT [15, 53] and Llama [67]. LLM is typically trained to optimize a conditional probability distribution $p(x_i|x_{<i})$ [24], which assigns a probability to each possible $x'_i \in \mathcal{D}$ given prefix tokens $x_{<i}$, where \mathcal{D} is the LLM vocabulary. Thus, the probability of the output sequence x [24, 58, 76] can be formulated as :

$$p(x) = \prod_{i=1}^q p(x_i|x_{<i}). \quad (1)$$

Notably, the probability of generating token x_i depends only on the prefix tokens $x_{<i}$, showing that LLMs are blind to the following tokens $x_{>i}$ after x_i .

2.2 Problem Formulation

Text-attributed graphs. A text-attributed graph (TAG) can be represented as $\mathcal{G} = (\mathcal{V}, \mathcal{E}, \mathcal{X}_v)$, where \mathcal{V} and \mathcal{E} denote the set of nodes and edges. $\mathcal{V} = \{v_1, v_2, \dots, v_n\}$ is the set of n nodes paired with raw text attributes $\mathcal{X} = \{\mathcal{X}_{v_1}, \mathcal{X}_{v_2}, \dots, \mathcal{X}_{v_n}\}$. $\mathcal{E} = \{e_{i,j}\}$ where $e_{i,j}$ is an edge from v_i to v_j . Particularly, for heterogeneous text-attributed graph, a TAG can be formulated as $\mathcal{G} = (\mathcal{V}, \mathcal{E}, \mathcal{X}_v, \mathcal{X}_e)$, where edges in \mathcal{E} are paired with raw text attributes $\mathcal{X}_e = \{\mathcal{X}_{e_{i,j}}\}$. The path in a TAG can be defined as $\mathcal{P} = (v_1, v_2, \dots, v_\ell)$, such that v_i is adjacent to v_{i+1} for $1 \leq i < \ell$. Such a path \mathcal{P} is called a path of length ℓ from v_1 to v_ℓ .

Shortest paths. Given a weighted graph $\mathcal{G} = (\mathcal{V}, \mathcal{E}, \mathcal{W})$, where $\mathcal{W} = \{w_{i,j}\}$ is the set of weights, each $e_{i,j} \in \mathcal{E}$ is paired with a positive real-valued weight $w_{i,j}$. Given two nodes $s, t \in \mathcal{V}$, the shortest path from s to t is the path $\mathcal{P} = (v_1, v_2, \dots, v_\ell)$ (where $v_1 = s$ and $v_\ell = t$) with the minimal weight sum $\sum_{i=1}^{\ell-1} w_{i,i+1}$. When

the graph is unweighted, we set each edge weight as 1, and the shortest path is equivalent to finding the path with the fewest edges.

Objective of Path-LLM. Given a text-attributed graph \mathcal{G} , the goal of Path-LLM is to generate unified graph embeddings ξ integrating complex graph structures and text attribute semantics in \mathcal{G} , and then improve task performances on multiple downstream tasks (e.g., node classification, link prediction and keyword search). Specifically, each node $v_i \in \mathcal{V}$ is paired with the embedding ξ_{v_i} extracted from Path-LLM.

3 Path-LLM MODEL

In this section, we introduce our Path-LLM model, which learns graph structures through *our proposed mechanism of L2SP selection and LLMs*. Figure 2 depicts the framework of Path-LLM with four key components in different phases, as follows.

- **Phase-I: L2SP selection.** To capture comprehensive graph properties, we first sample a few shortest paths of long length widely across the whole network and then cut them into short paths. We construct these long-to-short shortest paths (L2SP) as a base set of important path-based features for Path-LLM.
- **Phase-II: Path textualization.** Next, we employ the path textual function to obtain L2SP-based texts, incorporating the properties of L2SP, with each text representing a single L2SP within the graph.
- **Phase-III: Path-LLM pre-training.** These L2SP-based texts form a comprehensive dataset and are subsequently fed into the Path-LLM for self-supervised pre-training. As the Path-LLM acquires the ability to generate L2SP-based texts, it inherently learns to generate L2SP-based shortest paths.
- **Phase-IV: Path-LLM embedding generation.** Finally, we utilize the frozen Path-LLM model to extract Path-LLM embeddings that combine shortest path-based graph features with deep semantic information derived from node text attributes.

3.1 Phase-I: L2SP Selection

Generally, a graph has complex structures composed of dense groups and interconnections among them. Capturing features of these dense groups and connections is vital. Hence, to effectively obtain the critical structure of dense groups and their cross-over

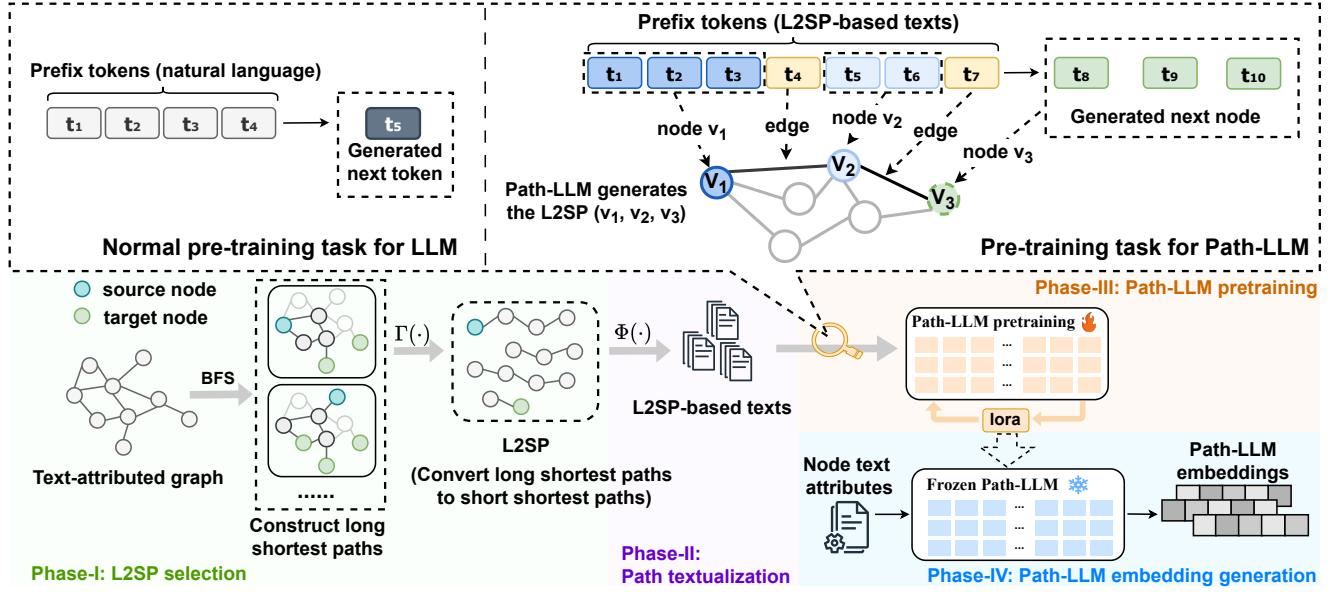


Figure 2: Our proposed Path-LLM framework involves four key components: (1) Long-to-short shortest path (L2SP) selection, converting sampled long shortest paths to L2SP-based shortest paths. (2) Path textualization, transforming L2SP-based shortest paths to L2SP-based texts. (3) Path-LLM pre-training, learning graph structures from L2SP-based texts. (4) Path-LLM embedding generation, deriving the final embeddings from the frozen Path-LLM.

connections, we first sample long paths \mathcal{P}_{long} from \mathcal{G} and then cut \mathcal{P}_{long} into small ones for easy learning by Path-LLM.

Long-path sampling. Randomly selecting a pair of nodes with a long shortest path between them is highly challenging, as many graphs have a small-world property. To effectively obtain \mathcal{P}_{long} , we propose a *fast long-path sampling algorithm*. We first randomly select a set $S = \{s_i\}_{i=1}^n$ of n nodes as the source nodes. A full-graph breadth-first search (BFS) [38] is then conducted for each source node s_i to identify nodes in \mathcal{G} at a distance greater than k edges from s_i . These identified nodes collectively form a candidate set $\mathcal{T}_i = \{\tau_{ij}\}_{j=1}^{n'}$ of target nodes, with the size of \mathcal{T}_i being n' . In other words, each node in \mathcal{T}_i is beyond the k -hop distance from s_i . Within this candidate set \mathcal{T}_i , a node is randomly chosen as the target node, denoted as τ_i . The BFS algorithm is then employed to find all long shortest paths between s_i and τ_i . To reduce the overlapping of these long paths, a subset of all long shortest paths is randomly selected to constitute the final result \mathcal{P}_{long} .

Long-to-short path conversion. To convert sampled long shortest paths \mathcal{P}_{long} into short ones, we propose the L2SP conversion method to cut them into short shortest-paths, denoted as $\Gamma(\mathcal{P}_{long})$. Given one long shortest path $\mathcal{P}_{long} = (v_1, v_2, \dots, v_L)$ and a parameter of maximum length ℓ , i.e., $\mathcal{P}_{short} = \{(v_{i+1}, \dots, v_{i+\ell}) | i = k(\ell - 1), 0 \leq k < \lfloor \frac{L}{\ell} \rfloor - 1\} \cup \{(v_{(\lfloor \frac{L}{\ell} \rfloor - 1)(\ell - 1) + 1}, \dots, v_L)\}$. For example, assume that a $\mathcal{P}_{long} = (v_1, v_2, v_3, v_4, v_5, v_6, v_7, v_8, v_9, v_{10})$ and $\ell = 3$, the output of $\Gamma(\mathcal{P}_{long})$ is a set of five shortest paths as $\mathcal{P}_{short} = \{(v_1, v_2, v_3), (v_3, v_4, v_5), (v_5, v_6, v_7), (v_7, v_8, v_9), (v_9, v_{10})\}$. Note that these five short paths can be connected via the cutting nodes, e.g., v_3, v_5, v_7 , and v_9 .

3.2 Phase-II: Path Textualization

To facilitate the Path-LLM's comprehension of our L2SP features, we utilize a path textual function to represent structural path into textual sequences, denoted as $\Phi(\cdot)$. Path textual function $\Phi(\cdot)$ can automatically concatenate node text attributes within the path \mathcal{P} to form the text sequence T , which can be formulated as $T = \Phi(\mathcal{P})$. $\Phi(\cdot)$ has different processing ways for two cases: homogeneous text-attributed graph and heterogeneous text-attributed graph, as shown in Figure 3. For homogeneous text-attributed graphs, we construct templates to join different text attributes better. $\Phi(\cdot)$ integrates templates and different text attributes into textual paths, as shown in Figure 3(a). For heterogeneous text-attributed graphs, given a path $\mathcal{P} = (v_1, v_2, \dots, v_\ell)$, $\Phi(\cdot)$ concatenates the text attributes of each node on the path as $\Phi(\mathcal{P}) = \langle \mathcal{X}_{v_1} | \mathcal{X}_{v_2} | \dots | \mathcal{X}_{v_\ell} \rangle$ to derive L2SP-based texts, as shown in Figure 3(b). Thus, we obtain the L2SP-based text by $T = \Phi(\mathcal{P})$, where $T = \{t_1, \dots, t_S\}$ and the length of one text is $|T| = S$.

Discussion. Our proposed path textual function $\Phi(\mathcal{P})$ differs from the textual path technique in WalkLM [66] due to WalkLM's inability to handle homogeneous graphs with abundant texts. Moreover, for heterogeneous graphs, WalkLM employs a rule-based program, which contrasts with our utilized concatenation method. Additionally, for nodes with excessively long text attributes, we conduct data cleaning and sentence segmentation, selecting essential sentences as the text attributes of the nodes. As a result, we obtained a dataset consisting of L2SP-based texts.

3.3 Phase-III: Path-LLM Pre-training

Based on the powerful semantic representation capabilities of LLM, Path-LLM integrates essential graph features in L2SP to its own

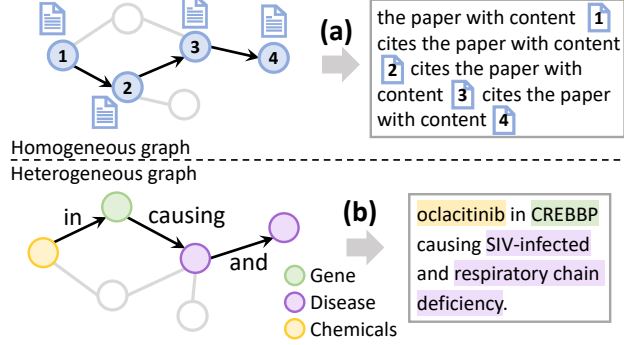


Figure 3: Path textualization.

deep semantic space. To achieve this, Path-LLM learns to generate L2SP-based texts constructed above through the self-supervised pre-training process. Specifically, we transform the order of nodes in the L2SP to the order of text tokens. As Path-LLM learns the order of tokens, it also learns the order of nodes within the L2SP.

Typically, the pre-training task for LLM is to generate the next token based on prefix tokens [15]. When Path-LLM generates L2SP-based texts, the pre-training task for Path-LLM is to generate the next node v_i on the corresponding L2SP based on prefix nodes $\{v_{<i}\}$. This process is then iteratively repeated until the whole L2SP is generated. Formally, the L2SP-based text can be denoted as $T = \Phi(\mathcal{P}) = \{\Phi(X_{v_i})\}$, where $1 \leq i \leq \ell$. $\Phi(X_{v_i})$ is the processed text attribute of the node v_i , and ℓ denotes the length of \mathcal{P} . Based on Eq. 1, the probability of Path-LLM predicting the next node X_{v_i} can be formulated as $p(\Phi(X_{v_i})|\Phi(X_{v_{<i}}))$. Thus, the probability of generating the whole shortest path \mathcal{P} is $p(\mathcal{P}) = \prod_{i=1}^{\ell} p(\Phi(X_{v_i})|\Phi(X_{v_{<i}}))$. Consequently, when Path-LLM generates unified graph embeddings, it can integrate the learned graph structure with its inherent deep semantic representation capabilities.

We use the cross-entropy loss function [82] during the self-supervised training process of Path-LLM. The L2SP-based text can also be denoted as $T = \{t_1, \dots, t_S\}$, where S denotes the length of T . Path-LLM starts generating from the first token t_1 and calculates the loss for generating the next token t_j based on prefix tokens $t_{<j}$. Therefore, the loss for generating one L2SP-based text is:

$$\mathcal{L}_{\text{pretrain-seq}} = \frac{1}{S} \sum_{j=1}^S \sum_{k=1}^{|\mathcal{D}|} y_k \log P_k(t_j|t_{<j}),$$

where j is the position in the sequence and k is the position in the LLM vocabulary \mathcal{D} . P_k represents the probability that the k -th token in \mathcal{D} is the next token, $|\mathcal{D}|$ denotes the size of the LLM vocabulary, and y_k is the label of whether the k -th token in \mathcal{D} is the token at position j . For the whole dataset composed of N L2SP-based texts, the final loss function is:

$$\mathcal{L}_{\text{pretrain}} = \frac{1}{N} \sum_N \mathcal{L}_{\text{pretrain-seq}},$$

3.4 Phase-IV: Path-LLM Embedding Generation

The node text attribute X_{v_i} can be a few words, a sentence, or a paragraph, all of which can be transformed into Path-LLM embeddings. Specifically, after cleaning and sentence segmenting X_{v_i} , we input $\Phi(X_{v_i})$ into the frozen Path-LLM and then extract all token

embeddings $\{\epsilon_i\}_{i=1}^x$ associated with the same node v_i , where x is the number of token embeddings from the same node. We extract embeddings from the last layer of the Path-LLM, where $\epsilon_i \in \mathbb{R}^d$ and d is the embedding dimension. To obtain the Path-LLM embedding for a specific node, the token embeddings related to the same node's text attribute are averaged, i.e., for a node v_i , the Path-LLM embedding $\xi_{v_i} \in \mathbb{R}^d$ is calculated as $\xi_{v_i} = \frac{1}{x} \sum_{i=1}^x \epsilon_i$. The embedding ξ_{v_i} integrates both the graph structure learned by Path-LLM and its inherent semantic understanding capabilities.

4 COMPARISON ANALYSIS

In this section, we analyze the advantages of our L2SP method in Phase-I and discuss the rationales of L2SP-based text generation in Phase-III.

4.1 Path Selection Analysis in Phase-I

We compare different choices of path selections and analyze their pros and cons, including 1) random walk v.s. shortest paths, 2) long paths v.s. short paths, and 3) random short paths v.s. our L2SP-based paths.

Random walk vs. Shortest paths. Previous work [66] applies random walk to sample paths, while it is less effective than our L2SP method in LLM due to three major reasons, *noisy and fragile*, *mismatching with LLM*, and *hardly covering bridge edges*.

First, random walk can easily involve noisy nodes and cycles, rendering them less robust. In contrast, the shortest path focuses on direct connections, *avoiding unnecessary detours through noisy nodes and cycles*. Thus, our methods demonstrate greater resilience to noisy nodes and other disruptions.

Second, random patterns may not match with the order of language sequences in LLM. *LLM may have limited ability to learn graph features from irregular random walks*. Most LLMs use causal language modeling (CLM) training techniques. LLMs generate tokens one by one according to the linguistic rules. The next token prediction is only based on the prefix tokens, not the following ones. Considering the prefix nodes in random walks, the next node is essentially random and unpredictable. Conversely, *the next node selection in the shortest path is also based on the prefix nodes*, making it more in line with the generation pattern of LLMs.

Last, random walk may hardly cover bridge edges, i.e., the edges across distinct dense groups. Consider a bridge formed by $w_1 - w_2 - w_3$ to connect two dense groups G_1 and G_2 shown in Figure 4. For a random source node s in a dense group, the generated random walk paths tend to stay within its dense groups, which misses the bridge $w_1 - w_2 - w_3$ as shown in Figure 4(a). On the other hand, L2SP-based shortest paths are converted from a long shortest path, where the source and target nodes that span a long distance may have a high probability of appearing in different dense groups, as shown in Figure 4(c). This easily enables to cover the bridge between dense groups by our L2SP-based path selection.

Long paths vs. Short paths. We compare two kinds of shortest paths in terms of different lengths, called as long path and short path, respectively. Given a long path $\mathcal{P} = (v_1, v_2, \dots, v_\ell)$, the distance between the source node v_1 and the target node v_ℓ is ℓ . LLM tends to learn from all the prefix nodes $(v_1, \dots, v_{\ell-1})$ and generate

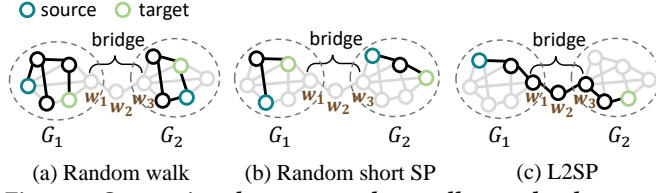


Figure 4: Comparison between random walks, randomly sampled short shortest paths, and L2SP-based paths.

the next node v_ℓ . A pair of nodes (v_1, v_ℓ) more than ℓ hops apart in a graph has a very weak relationship. However, the node embedding of v_ℓ still may be affected by the weakly associated node v_1 because LLM generates the next token based on all forward nodes. Therefore, we chose short shortest paths instead to avoid such irrelevant propagation.

Random short paths vs. L2SP-based paths. Similar to random walk, most randomly sampled shortest paths tend to fall within dense groups in Figure 4(b). It is also challenging to cover bridge edges by random shortest paths. Differently, our L2SP method could cover not only the paths in dense groups but also the interconnections between diverse dense groups. Overall, *L2SP-based shortest paths have more representative abilities as graph features.*

4.2 Rationales of Pre-training in Phase-III

During the Path-LLM pre-training process, L2SP-based text generation can be regarded as L2SP generation. Formally, the L2SP-based text can be denoted as $T = \Phi(\mathcal{P}) = \{\Phi(\mathcal{X}_{v_i})\} = \{t_j^{v_i}\}$, where $1 \leq j \leq S$ and $1 \leq i \leq \ell$. j represents the token index in T , while i represents the node index in the corresponding path. S is the length of the text, and ℓ is the length of the corresponding L2SP. Tokens associated to node v_i can be denoted as $\{t_{j^* \leq j \leq \bar{j}}^{v_i}\}$, where $t_{j^*}^{v_i}$ is the first token in $\Phi(\mathcal{X}_{v_i})$ and $t_{\bar{j}}^{v_i}$ is the last token in $\Phi(\mathcal{X}_{v_i})$. The probability of Path-LLM generating text attributes $\Phi(\mathcal{X}_{v_i})$ of node v_i [58, 76] is $\prod_{j=j^*}^{\bar{j}} p(t_j^{v_i} | t_{<j}^{v_{\leq i}})$, where $t_{<j}^{v_{\leq i}}$ represents a token list satisfying the token index being less than j and the node index being less than or equal to i . Then, we can formulate the probability of generating the L2SP-based text T as $\prod_{i=1}^{\ell} \prod_{j=j^*}^{\bar{j}} p(t_j^{v_i} | t_{<j}^{v_{\leq i}})$, while the probability of the corresponding L2SP generation can be formulated as $\prod_{i=1}^{\ell} p(\mathcal{X}_{v_i} | \mathcal{X}_{v_{<i}})$.

LEMMA 4.1. *During the Path-LLM pre-training process, L2SP-based text generation can be regarded as the L2SP generation. Formally,*

$$\prod_{i=1}^{\ell} \prod_{j=j^*}^{\bar{j}} p(t_j^{v_i} | t_{<j}^{v_{\leq i}}) = \prod_{i=1}^{\ell} p(\Phi(\mathcal{X}_{v_i}) | \Phi(\mathcal{X}_{v_{<i}})).$$

Based on Lemma 4.1, we can get that the process of Path-LLM generating L2SP-based texts is similar to the process of generating L2SP-based shortest paths. The proof details are in Appendix A.2.

5 PATH-LLM BASED KEYWORD SEARCH

To illustrate the usefulness of Path-LLM, we investigate the application of our learned Path-LLM embeddings to help tackle one typical graph analytics task of keyword search.

Keyword search. Keyword search is a classical graph query processing task widely applied in databases and recommendation systems [39, 69]. Given a graph G associated with node keywords and a set of query keywords Q , the goal of keyword search is to find the best subgraph H of G such that H covers all keywords Q and has the smallest edge weights. Following [78], we formulate the problem as follows. Given a weighted graph $\mathcal{G} = (V, E, W)$ a set of query keywords $Q = \{q_1, \dots, q_m\}$, the problem returns a tree structure $T \subseteq \mathcal{G}$, such that

- (1) V_T covers all keywords in Q ;
- (2) the edge weight $f(T)$ is minimized among all feasible choices, where $f(T) = \sum_{e_{i,j} \in E_T} w_{i,j}$.

However, in many real-world applications of keyword search, it strictly follows the original structure of given graphs but neglects the semantic connections of node weights, which limits the discovery of real close subgraph patterns w.r.t. the given keywords. Even worse, in some cases, the edge weights are not given in advance for the querying graph. In this paper, we *leverage the Path-LLM embedding to reconstruct a new weighted graph $\mathcal{G}^*(V, E^*, W^*)$ and search for an integrated keyword answer with close connections in terms of both topology structure and node semantics.*

Graph structure construction. Given a TAG $\mathcal{G}(V, E)$, we construct a new structure of graph \mathcal{G}^* based on the Path-LLM node embedding. Specifically, we first collect all isolated nodes V and then add edges into them as follows. For an edge $(v_i, v_j) \in E$, we measure its importance by calculating cosine-similarity [65] based on their embedding vectors ξ_i, ξ_j derived from Path-LLM, i.e.,

$$\psi_{i,j} = \frac{\xi_i \cdot \xi_j}{\|\xi_i\| \|\xi_j\|}, \text{ where } \psi_{i,j} \in [-1, 1]. \quad (2)$$

For $\psi_{i,j} < 0$, we consider ξ_i and ξ_j to be dissimilar, which is treated as the minimum non-negative edge weight of 0. Thus, we design a mapping function f^* as:

$$f^*(e_{i,j}) = \begin{cases} 0 & \text{for } \psi_{i,j} \leq 0 \\ \psi_{i,j} & \text{for } \psi_{i,j} > 0. \end{cases} \quad (3)$$

Only for a positive weight $\psi_{i,j}$, we add an edge connection between v_i and v_j . Thus, the new edge set is $E^* = \{e_{i,j} : v_i, v_j \in V, f^*(e_{i,j}) > 0\}$. Therefore, we obtain the topology structure V and E^* of new TAG \mathcal{G}^* without weights.

Edge importance weights assignment in \mathcal{G}^* . To find the most important subgraph T satisfying the requirements of both with minimum edges and semantically strongest related, covering all keywords in Q , we assign edge weights based on edge importance values. Considering one subgraph T , the importance of T is measured as the product of all edge importance values in T , i.e., $\prod_{e_{i,j} \in E_T} f^*(e_{i,j})$. Next, we convert the edge importance to the edge weight as $w_{i,j}^* = -\log f^*(e_{i,j})$, there by transforming our keyword search task into traditional keyword search task as follows,

$$\min \sum_{e_{i,j} \in E_T} w_{i,j}^* = \min \sum_{e_{i,j} \in E_T} -\log f^*(e_{i,j}) \Leftrightarrow \max \prod_{e_{i,j} \in E_T} f^*(e_{i,j})$$

Table 1: Statistics of tested datasets.

Dataset	Statistics of graphs			The number of training paths		
	#Nodes	#Edges	Graph type	#RW-paths [66]	#L2SP-paths	#L2SP-paths/#RW-paths
PubMed	63,109	244,986	heterogeneous graph	295,512	19,670	6.65%
Cora	2,708	5,429	homogeneous graph	100,000	12,922	12.92%
Citeseer	3,312	8,554	homogeneous graph	100,000	11,480	11.48%
OGB-ARXIV	169,343	1,166,243	homogeneous graph	350,000	28,698	8.19%

The goal of finding traditional Steiner Tree is $\min \sum_{e_{i,j} \in E_T} w_{i,j}^*$, the same as finding the most important subtree T , $\max \prod_{e_{i,j} \in E_T} f^*(e_{i,j})$. As a result, we finally obtain a new weighted TAG $\mathcal{G}^*(V, E^*, W^*)$. Across this TAG, we can search the subtree that satisfies both the fewest edges and semantically strongest related.

Our solution of keyword search over \mathcal{G}^* . We first consider one simple case of keyword search with $|Q| = 2$ for two query nodes v_i, v_j . We use Dijkstra’s algorithm [14] to search for the shortest path between v_i and v_j based on the new weight W^* . For a general keyword search with $|Q| \geq 3$, we adopt a 2-approximation greedy algorithm [51] for finding a Steiner Tree to cover all keywords Q to tackle this NP-hard problem.

6 EXPERIMENTS

Datasets. We evaluate on four datasets: Cora [50], Citeseer [18], PubMed [59], and ARXIV [28]. PubMed is a biomedical network containing four types of nodes: genes, diseases, chemicals, and species [77]. The other three datasets are citation networks with text attributes like title, abstract, and so on. Raw text data of Cora and Citeseer are collected from [11]. The detailed statistics are shown in Table 1. PubMed is a heterogeneous graph, while others are homogeneous graphs. Due to the limited space, experimental results of Citeseer and ARXIV are reported in Appendix A.4.

Competitive methods. We compare our proposed Path-LLM with SOTA GNN-, LM- and LLM-based methods as follows,

- **Three classical graph learning models:** We test three methods GCN [36], GraphSage [22], and GATv2 [5]. The GATv2 [5] proposes a dynamic graph attention variant and captures more expressive graph structures.
- **WalkLM [66]:** WalkLM is the state-of-the-art LM-based method, integrating random walks and RoBERTa [47] for unified graph representation learning.
- **Llama 2-7B [67]:** For a fair comparison, we also compare our method with the widely used large language model, Llama 2-7B, for graph embeddings with exceptionally powerful semantic representation abilities.

To assess the effectiveness of different graph embeddings, we only use a single-layer MLP as a classifier for node classification and link prediction in a more rigorous setting devoid of any supplementary models used in WalkLM. The different settings are detailed in Appendix A.3. All models are optimized through the Adam optimizer [35] with an initial learning rate of $2e-4$. The rank and scaling factor of the LoRA adapter [27] are set to 8 and 16. The length of the long shortest path is set to $k = 10$ for particular social networks with an average distance of $4 \sim 7$. Table 1 also reports the number of paths used in training data for WalkLM and L2SP, respectively. As an effective learning model, our L2SP method uses much fewer shortest paths than the number of random-walk-based paths in WalkLM [66], which reduces 90.19% of paths on average for four

datasets. All experiments are implemented by PyTorch with two NVIDIA A100(80G) GPUs.

6.1 Node Classification

For node classification, we train a separate one-layer MLP classifier based on all unified graph embeddings and evaluate graph embeddings derived from all methods with Macro-F1 (across all labels) and Micro-F1 (across all nodes) [20]. Note that for GNNs, we train GNNs through contrastive learning to generate unified graph embeddings and then feed them into MLP for downstream tasks.

As shown in Table 2, our proposed Path-LLM has superior performance on PubMed and Cora. Our proposed Path-LLM showcases substantial performance enhancements over WalkLM and other GNN-based and LM-based competitors. For PubMed, Path-LLM achieves a remarkable 175.67% performance gain in macro-F1 and 103.63% in micro-F1 over WalkLM. Moreover, Path-LLM outperforms WalkLM by achieving a 72.58% performance gain in macro-F1 and 36.82% in micro-F1 on Cora. In addition, it demonstrates that the shortest path structure can significantly enhance the effectiveness of Path-LLM, with an average 4.31% gain of the pure LLM method Llama 2 [67] on PubMed and an average 5.2% gain of Llama 2 [67] on Cora, verifying that the structural information learned by Path-LLM is beneficial for node classification.

6.2 Link Prediction

For link prediction, we use the Hadamard function to construct feature vectors for node pairs and train a two-layer MLP classifier on the selected links. We evaluate graph embeddings with AUC (area under the ROC curve) and Accuracy [30]. Note that for GNNs, we use GNNs to generate graph embeddings and then construct feature vectors for node pairs. Table 2 shows that our Path-LLM achieves remarkable performance in uncovering latent associations among nodes in text-attributed graphs. This implies that Path-LLM possesses a more precise grasp of graph structure through semantic information integration, thus conferring advantages in link prediction tasks. Path-LLM consistently outperforms WalkLM, achieving a notable 23.48% performance gain in macro-F1 and 22.11% in micro-F1 on PubMed. Meanwhile, Path-LLM achieves a notable 3.96% performance gain in AUC and 4.75% in accuracy over WalkLM on Cora. Compared to pure LLM, the structural advantages displayed by the L2SP on PubMed is an average 3.6% increase and an average 4.43% increase on Cora.

6.3 Ablation Studies

We perform an ablation study to verify the effectiveness of our proposed L2SP structure in Section 4.1, compared to other path structures. To conduct a comprehensive evaluation, we propose several baselines for ablation study: LLM with 1-hop neighbors, LLM with random walk, LLM with new (α, β, γ) random walk [46],

Table 2: The results of node classification and link prediction on PubMed and Cora datasets.

Datasets	PubMed				Cora			
Tasks	Node classification		Link prediction		Node classification		Link prediction	
Metrics	Macro-F1	Micro-F1	AUC	Accuracy	Macro-F1	Micro-F1	AUC	Accuracy
GCN [36]	0.2593	0.3570	0.5155	0.5426	0.3628	0.4040	0.6680	0.7018
GraphSage [22]	0.2140	0.2430	0.5133	0.5211	0.3684	0.4140	0.7445	0.4052
GATv2 [5]	0.2501	0.2870	0.5204	0.5011	0.3706	0.4740	0.5143	0.4488
WalkLM [66]	0.2721	0.3699	0.5962	0.5684	0.4031	0.5336	0.8581	0.7746
Llama 2 [67]	0.7167	0.7246	0.7144	0.6665	0.6608	0.6946	0.8568	0.7809
Path-LLM (Ours)	0.7501	0.7532	0.7362	0.6941	0.6957	0.7301	0.8921	0.8114

Table 3: Ablation study: Experimental results of different path structures involving 1-hop neighbors, random walks (RW), (α, β, γ) RW, randomly sampled short shortest paths and long shortest paths.

Datasets	PubMed				Cora			
Tasks	Node classification		Link prediction		Node classification		Link prediction	
Metrics	Macro-F1	Micro-F1	AUC	Accuracy	Macro-F1	Micro-F1	AUC	Accuracy
LLM	0.7167 (-3.34%)	0.7246 (-2.86%)	0.7144 (-2.18%)	0.6665 (-2.76%)	0.6608 (-3.49%)	0.6946 (-3.55%)	0.8568 (-3.56%)	0.7809 (-3.05%)
LLM + 1hop	0.7219 (-2.82%)	0.7378 (-1.54%)	0.6534 (-8.28%)	0.6126 (-8.15%)	0.6734 (-2.23%)	0.7045 (-2.56%)	0.8709 (-2.12%)	0.7913 (-2.01%)
LLM + RW	0.7233 (-2.68%)	0.7356 (-1.76%)	0.6424 (-9.38%)	0.6041 (-9.00%)	0.6689 (-2.68%)	0.7012 (-2.89%)	0.8728 (-1.93%)	0.7892 (-2.22%)
LLM + (α, β, γ) RW [46]	0.7212 (-2.89%)	0.7378 (-1.54%)	0.6632 (-7.30%)	0.6240 (-7.01%)	0.6752 (-2.05%)	0.7067 (-2.34%)	0.8753 (-1.68%)	0.7981 (-1.33%)
LLM + Random Short	0.7284 (-2.17%)	0.7422 (-1.10%)	0.6555 (-8.07%)	0.6145 (-7.96%)	0.6742 (-2.15%)	0.7082 (-2.19%)	0.8860 (-0.61%)	0.8056 (-0.58%)
LLM + Long SP	0.7297 (-2.04%)	0.7445 (-0.87%)	0.6587 (-7.75%)	0.6190 (-7.51%)	0.6691 (-2.66%)	0.7053 (-2.48%)	0.8776 (-1.45%)	0.8007 (-1.07%)
LLM + L2SP	0.7501	0.7532	0.7362	0.6941	0.6957	0.7301	0.8921	0.8114

Table 4: Ablation study of the L2SP and long shortest path.

Datasets	PubMed			
Tasks	Node classification		Link prediction	
Metrics	Macro-F1	Micro-F1	AUC	Accuracy
long num1	0.7359	0.7488	0.6484	0.6137
L2SP num1	0.7529	0.7644	0.6866	0.6451
long num5	0.7223	0.7357	0.6736	0.6332
L2SP num5	0.7471	0.7555	0.7497	0.7111
long num10	0.7297	0.7445	0.6587	0.6190
L2SP num10	0.7501	0.7532	0.7362	0.6941

LLM with long shortest path and LLM with randomly sampled short shortest path. Particularly, when reproducing (α, β, γ) random walk, we utilize Sentence-BERT [57] to process node embeddings. Here, we present findings from PubMed and Cora. Results for the remaining two datasets can be found in the Appendix A.5.

Ablation Study 1: Different path structures. Table 3 compares the effectiveness of different graph embeddings with distinct path structures on node classification and link prediction. It is evident that the shortest path structure outperforms the random walk structure, even superior to the new (α, β, γ) random walk with an average increase of 3.97% on PubMed and 3.18% on Cora for node classification. Especially in link prediction, which evaluates the graph structure understanding of LLMs, the results show that the different path structures influence LLMs’ learning of the graph structure. RW-based LLM even decreases 10.08% of AUC after training with random walks. Our proposed L2SP-based structure yields the best results among all methods, with 12.31% performance gains in AUC and 12.95% accuracy over randomly sampled shortest paths on PubMed.

Ablation Study 2: L2SP-based shortest paths outperform long shortest paths. We evaluate whether L2SP is better than the original long shortest path for the case of different sampling paths. For

several types of shortest paths between the same pair of nodes, we sampled 1, 5, and 10 longest shortest paths, respectively, to verify whether the effectiveness of L2SP-based shortest paths is better than long shortest paths. Table 4 shows that the L2SP perform better than the long shortest path with an average 2.84% gain in macro-f1 and 1.98% gain in micro-f1 for node classification while an average 9.65% in AUC and 9.85% in accuracy for link prediction. **Ablation Study 3: L2SP’s structural advantage is significant in graphs with fewer text attributes.** Due to the limited space, the details of the analysis are reported in Appendix A.5.

6.4 Case Study of Keyword Search

We conduct a case study of keyword search by comparing three graph weighting methods, including the uniform weights, WalkLM-based weights, and our Path-LLM-based weights. This aims to evaluate the effectiveness of Path-LLM weights to find tight groups in terms of graph structure and node semantics. Our comprehensive case study thoroughly explores the inherent benefits of Path-LLM concerning both graph structure and semantics on PubMed. Figure 5 shows Steiner trees based on four given keywords $Q = \{q_1: \text{hepatocellular}, q_2: \text{craniofacial anomalies}, q_3: \text{attention impairment}, q_4: \text{intra-uterine}\}$. In terms of graph structure perspective, the Path-LLM-based weight obtains the fewest five edges and the closest ties between nodes. In contrast, graphs generated with uniform and WalkLM-based weights are sparser, with longer and less tight connections between nodes, like the association between the nodes $\{w_5: \text{acromegaly}\}$ and $\{w_6: \text{impaired glucose homeostasis}\}$. In terms of node semantics perspective, the Path-LLM-based weighted subtree contains rich and medically proven associations. To elaborate, the occurrence of (q_1) hepatocellular issues along with symptoms of (q_2) craniofacial anomalies is highly indicative of the presence of (w_5) acromegaly [1, 8]. (w_5) may lead to (w_6) impaired glucose

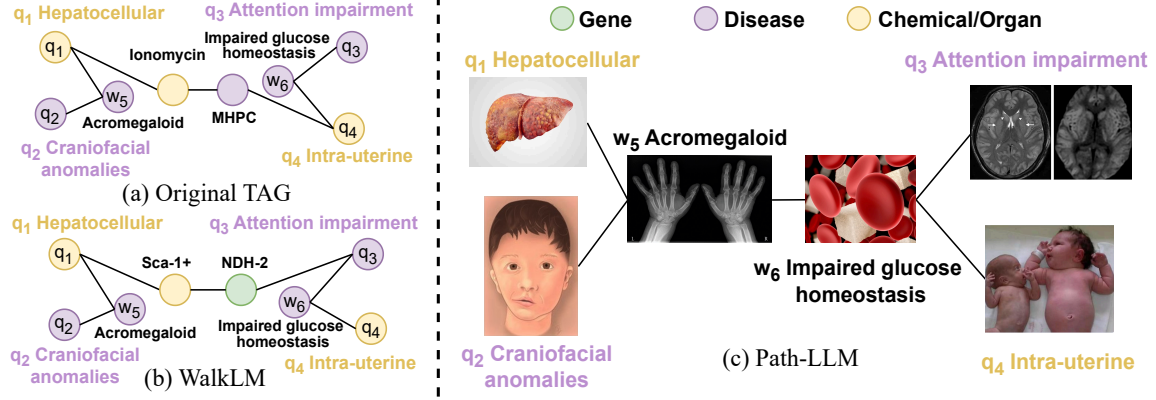


Figure 5: Case study of keyword search with a query $Q = \{q_1: \text{hepatocellular}, q_2: \text{craniofacial anomalies}, q_3: \text{attention impairment}, q_4: \text{intra-uterine}\}$. Path-LLM finds a semantically meaningful answer with the smallest number of five edges.

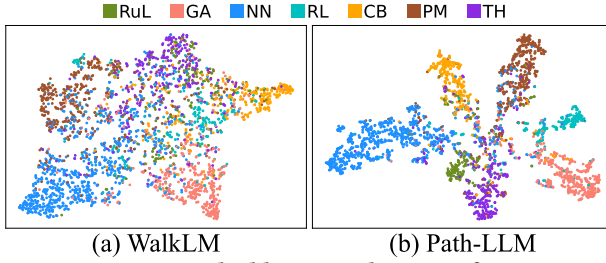


Figure 6: Embedding visualization of Cora.

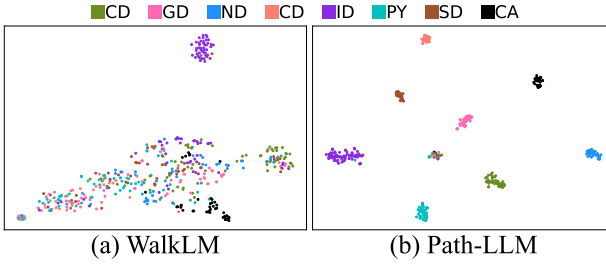


Figure 7: Embedding visualization of PubMed.

homeostasis [7, 10] with potential risks of (q_3) attention impairment causing by brain damage [3, 34, 63] and (q_4) intra-uterine growth retardation [17, 37, 52]. In contrast, subtrees derived from uniform and WalkLM-based weights exhibit weaker semantic associations between nodes and lack strong medical evidence.

6.5 Visualization of Path-LLM Embeddings

For an intuitive comparison, we visualize the embedding space of different types of nodes learned by WalkLM and our proposed Path-LLM on Cora and PubMed, respectively. The embeddings are further transformed into the 2-dimensional Euclidean space via the t-SNE [12]. The nodes are colored according to their types. Figures 6 and 7 show that node representations derived from our Path-LLM are more discriminative from different classes than WalkLM.

7 RELATED WORK

In recent years, various graph representation learning approaches have been studied [33, 43, 45, 61, 70].

GNN-based graph representation learning. Graph neural networks (GNNs) have been employed to learn representations

by aggregating information from neighboring nodes on graphs [22, 36, 41, 68, 73, 81, 84, 85]. Some studies [29, 32, 48, 79] have utilized self-supervision techniques to pre-train a sophisticated GNN model for unified graph embedding learning, such as contrastive learning. However, this method predominantly focuses on the graph structure, leading to shallow and rough alignment of semantic information and insufficient integration of structural and semantic information.

LM-based graph representation learning. Several studies have employed diverse methodologies to generate graph embeddings using Language Models (LM) [19, 24, 25, 42, 44, 66, 71, 83]. GLEM [83] employs an expectation-maximization approach to integrate GNNs and LMs for node classification. To enhance GLEM [83], TAPE [24] utilizes an LLM to provide additional information and leverages LMs to generate embeddings. However, GLEM [83] and TAPE [24] can only handle citation networks, and the graph embeddings generated by the language model can only be used for node classification, not for generating unified graph representations. ZeroG [44] combines graph prompts with LM to solve the problem of zero-shot transferability, which does not solve unified graph representation learning. Currently, the state-of-the-art approach, WalkLM [66], still utilizes LM to generate embeddings, which is markedly inferior to that of LLM [56, 64], such as GPT-4 [53] and Llama [67]. *Different from most existing studies, our emphasis is to generate unified embeddings for each node to capture both its topological and semantic features. Our learning model leverages advanced LLMs and well-developed shortest path selection to tackle graph learning tasks and NP-hard graph querying task of keyword search.*

8 CONCLUSIONS

In this paper, we propose a novel Path-LLM model for unified graph representation learning. The key design of our model involves a sampled selection of our proposed L2SP-based shortest paths to represent the whole network. Then, we utilize a large language model to integrate graph structure to deep semantic embedding space by learning our L2SP-based texts. We develop techniques to construct a new weighted graph based on Path-LLM-based embedding and tackle a NP-hard graph querying task of keyword search by finding better answers. Comprehensive experiments validate the effectiveness of our Path-LLM model and embeddings.

REFERENCES

- [1] Amit Akirov, Hiba Masri-Iraqi, Idit Dotan, and Ilan Shimon. 2021. The biochemical diagnosis of acromegaly. *Journal of clinical medicine* 10, 5 (2021), 1147.
- [2] Paolo G Arduino, Marco Cabras, Giovanni Lodi, and Stefano Petti. 2022. Herpes simplex virus type 1 in subgingival plaque and periodontal diseases. Meta-analysis of observational studies. *Journal of Periodontal Research* 57, 2 (2022), 256–268.
- [3] ROLAND N Auer. 1986. Progress review: hypoglycemic brain damage. *Stroke* 17, 4 (1986), 699–708.
- [4] Andrei Broder, Ravi Kumar, Farzin Maghoul, Prabhakar Raghavan, Sridhar Rajagopalan, Raymie Stata, Andrew Tomkins, and Janet Wiener. 2000. Graph structure in the web. *Computer networks* 33, 1–6 (2000), 309–320.
- [5] Shaked Brody, Uri Alon, and Eran Yahav. 2022. How Attentive are Graph Attention Networks?. In *The Tenth International Conference on Learning Representations, ICLR 2022, Virtual Event, April 25–29, 2022*. OpenReview.net.
- [6] Peggy Bruynseels, Philippe G Jorens, Hendrik E Demey, Herman Goossens, Stefaan R Pattyn, Monique M Elseviers, Joost Weyler, Leo L Bossaert, Yves Mentens, and Margareta Ieven. 2003. Herpes simplex virus in the respiratory tract of critical care patients: a prospective study. *The Lancet* 362, 9395 (2003), 1536–1541.
- [7] John D Carmichael, Vivien S Bonert, James M Mirocha, and Shlomo Melmed. 2009. The utility of oral glucose tolerance testing for diagnosis and assessment of treatment outcomes in 166 patients with acromegaly. *The Journal of Clinical Endocrinology & Metabolism* 94, 2 (2009), 523–527.
- [8] John D Carmichael, Michael S Broder, Dasha Cherepanov, Eunice Chang, Adam Mamelak, Qayyim Said, Maureen P Neary, and Vivien Bonert. 2017. The association between biochemical control and cardiovascular risk factors in acromegaly. *BMC endocrine disorders* 17 (2017), 1–6.
- [9] Rudolf Carnap. 1962. *Logical foundations of probability*. Vol. 2. CiteSeer.
- [10] Beatriz M Chang-DeMoranville and Ivor MD Jackson. 1992. Diagnosis and endocrine testing in acromegaly. *Endocrinology and metabolism clinics of North America* 21, 3 (1992), 649–668.
- [11] Zhikai Chen, Haitao Mao, Hang Li, Wei Jin, Hongzhi Wen, Xiaochi Wei, Shuaiqiang Wang, Dawei Yin, Wenqi Fan, Hui Liu, and Jiliang Tang. 2023. Exploring the Potential of Large Language Models (LLMs) in Learning on Graphs. *SIGKDD Explor.* 25, 2 (2023), 42–61.
- [12] Laurens Van der Maaten and Geoffrey Hinton. 2008. Visualizing data using t-sne. *Journal of Machine Learning Research* 9 (2008), 2579–2605.
- [13] Jacob Devlin, Ming-Wei Chang, Kenton Lee, and Kristina Toutanova. 2019. BERT: Pre-training of Deep Bidirectional Transformers for Language Understanding. In *Proceedings of the 2019 Conference of the North American Chapter of the Association for Computational Linguistics: Human Language Technologies, Volume 1 (Long and Short Papers)*. 4171–4186.
- [14] Edsger W. Dijkstra. 1959. A note on two problems in connexion with graphs. *Numer. Math.* 1 (1959), 269–271.
- [15] Luciano Floridi and Massimo Chiriacchi. 2020. GPT-3: Its nature, scope, limits, and consequences. *Minds and Machines* 30 (2020), 681–694.
- [16] Jared R Gallaher and Anthony Charles. 2022. Acute cholecystitis: a review. *Jama* 327, 10 (2022), 965–975.
- [17] Maria G Vemes, Sofia Asim Rahman, Ritika R Kapoor, Sarah Flanagan, Jayne AL Houghton, Shivani Misra, Nick Oliver, Mehul Tulsidas Dattani, and Pratik Shah. 2020. Hyperinsulinemic hypoglycemia in children and adolescents: recent advances in understanding of pathophysiology and management. *Reviews in Endocrine and Metabolic Disorders* 21 (2020), 577–597.
- [18] C. Lee Giles, Kurt D. Bollacker, and Steve Lawrence. 1998. CiteSeer: An Automatic Citation Indexing System. In *Proceedings of the 3rd ACM International Conference on Digital Libraries, June 23–26, 1998, Pittsburgh, PA, USA*. ACM, 89–98.
- [19] Justin Gilmer, Samuel S Schoenholz, Patrick F Riley, Oriol Vinyals, and George E Dahl. 2017. Neural message passing for quantum chemistry. In *International Conference on Machine Learning*. PMLR, 1263–1272.
- [20] Cyril Goutte and Éric Gaussier. 2005. A Probabilistic Interpretation of Precision, Recall and F-Score, with Implication for Evaluation. In *Advances in Information Retrieval, 27th European Conference on IR Research (Lecture Notes in Computer Science, Vol. 3408)*. Springer, 345–359.
- [21] Peter J Gruber, Robert A Silverman, Steven Gottesfeld, and Edith Flaster. 1996. Presence of fever and leukocytosis in acute cholecystitis. *Annals of emergency medicine* 28, 3 (1996), 273–277.
- [22] William L. Hamilton, Zhitaoying, and Jure Leskovec. 2017. Inductive Representation Learning on Large Graphs. In *Advances in Neural Information Processing Systems 30: Annual Conference on Neural Information Processing Systems 2017, December 4–9, 2017, Long Beach, CA, USA*. 1024–1034.
- [23] Pengcheng He, Xiaodong Liu, Jianfeng Gao, and Weizhu Chen. 2020. DEBERTA: DECODING-ENHANCED BERT WITH DISENTANGLED ATTENTION. In *International Conference on Learning Representations*.
- [24] Xiaoxin He, Xavier Bresson, Thomas Laurent, Adam Perold, Yann LeCun, and Bryan Hooi. 2023. Harnessing explanations: Llm-to-lm interpreter for enhanced text-attributed graph representation learning. *arXiv preprint arXiv:2305.19523* (2023).
- [25] Roei Herzig, Alon Mendelson, Leonid Karlinsky, Assaf Arbel, Rogério Feris, Trevor Darrell, and Amir Globerson. 2023. Incorporating Structured Representations into Pretrained Vision & Language Models Using Scene Graphs. In *Proceedings of the 2023 Conference on Empirical Methods in Natural Language Processing*. Association for Computational Linguistics, 14077–14098.
- [26] Yuning Hong, Jacky WY Lam, and Ben Zhong Tang. 2009. Aggregation-induced emission: phenomenon, mechanism and applications. *Chemical communications* 29 (2009), 4332–4353.
- [27] Edward J. Hu, Yelong Shen, Phillip Wallis, Zeyuan Allen-Zhu, Yuanzhi Li, Shean Wang, Lu Wang, and Weizhu Chen. 2022. LoRA: Low-Rank Adaptation of Large Language Models. In *The Tenth International Conference on Learning Representations, ICLR 2022, Virtual Event, April 25–29, 2022*. OpenReview.net. <https://openreview.net/forum?id=nZeVKeeFYf9>
- [28] Weihua Hu, Matthias Fey, Marinka Zitnik, Yuxiao Dong, Hongyu Ren, Bowen Liu, Michele Catasta, and Jure Leskovec. 2020. Open Graph Benchmark: Datasets for Machine Learning on Graphs. In *Advances in Neural Information Processing Systems 33: Annual Conference on Neural Information Processing Systems*.
- [29] Ziniu Hu, Yuxiao Dong, Kuansan Wang, Kai-Wei Chang, and Yizhou Sun. 2020. GPT-GNN: Generative Pre-Training of Graph Neural Networks. In *The 26th ACM SIGKDD Conference on Knowledge Discovery and Data Mining, Virtual Event, CA, USA, August 23–27, 2020*. ACM, 1857–1867.
- [30] Jin Huang and Charles X. Ling. 2005. Using AUC and Accuracy in Evaluating Learning Algorithms. *IEEE Trans. Knowl. Data Eng.* 17, 3 (2005), 299–310.
- [31] Ana Vitoria Imbroni, Osmar Shizuo Okuda, Nivea Maria de Freitas, Roberto Fraga Moreira Lotufo, and Fabio Daumas Nunes. 2008. Detection of herpesviruses and periodontal pathogens in subgingival plaque of patients with chronic periodontitis, generalized aggressive periodontitis, or gingivitis. *Journal of periodontology* 79, 12 (2008), 2313–2321.
- [32] Xunqiang Jiang, Tianrui Jia, Yuan Fang, Chuan Shi, Zhe Lin, and Hui Wang. 2021. Pre-training on Large-Scale Heterogeneous Graph. In *The 27th ACM SIGKDD Conference on Knowledge Discovery and Data Mining, Virtual Event, Singapore, August 14–18, 2021*. Feida Zhu, Beng Chin Ooi, and Chunyan Miao (Eds.). ACM, 756–766.
- [33] Wei Ju, Zheng Fang, Yiyang Gu, Zequn Liu, Qingqing Long, Ziyue Qiao, Yifang Qin, Jianhao Shen, Fang Sun, Zhiping Xiao, Junwei Yang, Jingyang Yuan, Yusheng Zhao, Yifan Wang, Xiao Luo, and Ming Zhang. 2024. A Comprehensive Survey on Deep Graph Representation Learning. *Neural Networks* 173 (2024), 106207.
- [34] Sanjay Kalra, Jagat Jyoti Mukherjee, Subramaniam Venkataraman, Ganapathi Bantwal, Shehla Shaikh, Banshi Saboo, Ashok Kumar Das, and Ambady Ramachandran. 2013. Hypoglycemia: The neglected complication. *Indian journal of endocrinology and metabolism* 17, 5 (2013), 819–834.
- [35] Diederik P. Kingma and Jimmy Ba. 2015. Adam: A Method for Stochastic Optimization. In *3rd International Conference on Learning Representations, Yoshua Bengio and Yann LeCun (Eds.)*. <http://arxiv.org/abs/1412.6980>
- [36] Thomas N. Kipf and Max Welling. 2017. Semi-Supervised Classification with Graph Convolutional Networks. In *5th International Conference on Learning Representations, ICLR 2017, Toulon, France, April 24–26, 2017, Conference Track Proceedings*. OpenReview.net.
- [37] Oded Langer, Karla Damus, Mitchell Maiman, Michael Divon, Judith Levy, and William Bauman. 1986. A link between relative hypoglycemia-hypoinsulinemia during oral glucose tolerance tests and intrauterine growth retardation. *American journal of obstetrics and gynecology* 155, 4 (1986), 711–716.
- [38] C. Y. Lee. 1961. An Algorithm for Path Connections and Its Applications. *IRE Trans. Electron. Comput.* 10, 3 (1961), 346–365.
- [39] Guoliang Li, Beng Chin Ooi, Jianhua Feng, Jianyong Wang, and Lizhu Zhou. 2008. Ease: an effective 3-in-1 keyword search method for unstructured, semi-structured and structured data. In *Proceedings of the 2008 ACM SIGMOD international conference on Management of data*. 903–914.
- [40] Min Li, Zhen Liu, Yuan Lin, Xinlin Chen, Shengli Li, Fengzhi You, Ying Deng, Nana Li, Yanping Wang, Yanqing Zhang, et al. 2014. Maternal influenza-like illness, medication use during pregnancy and risk of congenital heart defects in offspring. *The Journal of Maternal-Fetal & Neonatal Medicine* 27, 8 (2014), 807–811.
- [41] Pan Li, Yanbang Wang, Hongwei Wang, and Jure Leskovec. 2020. Distance encoding: Design provably more powerful neural networks for graph representation learning. *Advances in Neural Information Processing Systems* 33 (2020), 4465–4478.
- [42] Yichuan Li, Kaize Ding, and Kyumin Lee. 2023. GRENADE: Graph-Centric Language Model for Self-Supervised Representation Learning on Text-Attributed Graphs. In *Findings of the Association for Computational Linguistics: EMNLP 2023, Singapore, December 6–10, 2023*. Association for Computational Linguistics, 2745–2757.
- [43] Yuhua Li, Zhixun Li, Peisong Wang, Jia Li, Xiangguo Sun, Hong Cheng, and Jeffrey Xu Yu. 2023. A survey of graph meets large language model: Progress and future directions. *arXiv preprint arXiv:2311.12399* (2023).
- [44] Yuhua Li, Peisong Wang, Zhixun Li, Jeffrey Xu Yu, and Jia Li. 2024. ZeroG: Investigating Cross-dataset Zero-shot Transferability in Graphs. *CoRR abs/2402.11235* (2024). [arXiv:2402.11235](https://arxiv.org/abs/2402.11235)

- [45] Yuhan Li, Peisong Wang, Xiao Zhu, Aochuan Chen, Haiyun Jiang, Deng Cai, Victor Wai Kin Chan, and Jia Li. 2024. GLBench: A Comprehensive Benchmark for Graph with Large Language Models. *arXiv preprint arXiv:2407.07457* (2024).
- [46] Yiran Li, Renchi Yang, and Jieming Shi. 2023. Efficient and Effective Attributed Hypergraph Clustering via K-Nearest Neighbor Augmentation. *Proc. ACM Manag. Data* 1, 2 (2023), 116:1–116:23.
- [47] Yinhan Liu, Mylène Ott, Naman Goyal, Jingfei Du, Mandar Joshi, Danqi Chen, Omer Levy, Mike Lewis, Luke Zettlemoyer, and Veselin Stoyanov. 2019. Roberta: A robustly optimized bert pretraining approach. *arXiv preprint arXiv:1907.11692* (2019).
- [48] Xiao Luo, Wei Ju, Yiyang Gu, Zhengyang Mao, Luchen Liu, Yuhui Yuan, and Ming Zhang. 2024. Self-supervised Graph-level Representation Learning with Adversarial Contrastive Learning. *ACM Trans. Knowl. Discov. Data* 18, 2 (2024), 34:1–34:23.
- [49] JM Luteijn, MJ Brown, and Helen Dolk. 2014. Influenza and congenital anomalies: a systematic review and meta-analysis. *Human reproduction* 29, 4 (2014), 809–823.
- [50] Andrew Kachites McCallum, Kamal Nigam, Jason Rennie, and Kristie Seymore. 2000. Automating the Construction of Internet Portals with Machine Learning. *Inf. Retr.* 3, 2 (2000), 127–163.
- [51] Kurt Mehlhorn. 1988. A faster approximation algorithm for the Steiner problem in graphs. *Inform. Process. Lett.* 27, 3 (1988), 125–128.
- [52] Edward S Ogata, Mary E Bussey, Andrew Labarbera, and Sandra Finley. 1985. Altered growth, hypoglycemia, hypocalcemia, and ketonemia in the young rat: postnatal consequences of intrauterine growth retardation. *Pediatric research* 19, 1 (1985), 32–37.
- [53] OpenAI. 2023. GPT-4 Technical Report. *CoRR* abs/2303.08774 (2023). *arXiv:2303.08774*
- [54] Matthew E Oster, Tiffany Riehle-Colarusso, Clinton J Alverson, and Adolfo Correa. 2011. Associations between maternal fever and influenza and congenital heart defects. *The Journal of pediatrics* 158, 6 (2011), 990–995.
- [55] Long Ouyang, Jeffrey Wu, Xu Jiang, Diogo Almeida, Carroll Wainwright, Pamela Mishkin, Chong Zhang, Sandhini Agarwal, Katarina Slama, Alex Ray, et al. 2022. Training language models to follow instructions with human feedback. *Advances in Neural Information Processing Systems* 35 (2022), 27730–27744.
- [56] Long Ouyang, Jeffrey Wu, Xu Jiang, Diogo Almeida, Carroll L. Wainwright, Pamela Mishkin, Chong Zhang, Sandhini Agarwal, Katarina Slama, Alex Ray, John Schulman, Jacob Hilton, Fraser Kelton, Luke Miller, Maddie Simens, Amanda Askell, Peter Welinder, Paul F. Christiano, Jan Leike, and Ryan Lowe. 2022. Training language models to follow instructions with human feedback. In *Advances in Neural Information Processing Systems 35: Annual Conference on Neural Information Processing Systems*.
- [57] Nils Reimers and Iryna Gurevych. 2019. Sentence-BERT: Sentence Embeddings using Siamese BERT-Networks. In *Proceedings of the 2019 Conference on Empirical Methods in Natural Language Processing and the 9th International Joint Conference on Natural Language Processing*. 3982–3992.
- [58] James Requeima, John F Bronskill, Dami Choi, Richard E Turner, and David Duvenaud. 2024. LLM Processes: Numerical Predictive Distributions Conditioned on Natural Language. In *ICML 2024 Workshop on In-Context Learning*.
- [59] Prithviraj Sen, Galileo Namata, Mustafa Bilgic, Lise Getoor, Brian Gallagher, and Tina Eliassi-Rad. 2008. Collective Classification in Network Data. *AI Mag.* 29, 3 (2008), 93–106.
- [60] Prithviraj Sen, Galileo Namata, Mustafa Bilgic, Lise Getoor, Brian Galligher, and Tina Eliassi-Rad. 2008. Collective classification in network data. *AI magazine* 29, 3 (2008), 93–93.
- [61] Wenbo Shang and Xin Huang. 2024. A Survey of Large Language Models on Generative Graph Analytics: Query, Learning, and Applications. *arXiv preprint arXiv:2404.14809* (2024).
- [62] Sorina Mihaela Solomon, Ana Maria Filioreanu, Carmen Gabriela Stelea, Simona Ionela Grigoras, Irina Georgeta Sufaru, George Alexandru Maftei, Silvia Martu, Mihaela Monica Scutariu, and Cristina Popa. 2018. The assessment of the association between herpesviruses and subgingival bacterial plaque by real-time PCR analysis. *Rev. Chim* 69, 2 (2018), 507–510.
- [63] Jun Su and Li Wang. 2012. Research advances in neonatal hypoglycemic brain injury. *Translational pediatrics* 1, 2 (2012), 108.
- [64] Lichao Sun, Yue Huang, Haoran Wang, Siyuan Wu, Qihui Zhang, Chujie Gao, Yixin Huang, Wenhan Lyu, Yixuan Zhang, Xiner Li, Zhengliang Liu, Yixin Liu, Yijue Wang, Zhikun Zhang, Bhavya Kailkhura, Caiming Xiong, Chaowei Xiao, Chunyuan Li, Eric P. Xing, Furong Huang, Hao Liu, Heng Ji, Hongyi Wang, Huan Zhang, Huaxiu Yao, Manolis Kellis, Marinka Zitnik, Meng Jiang, Mohit Bansal, James Zou, Jian Pei, Jian Liu, Jianfeng Gao, Jiawei Han, Jieyu Zhao, Jiliang Tang, Jindong Wang, John Mitchell, Kai Shu, Kaidi Xu, Kai-Wei Chang, Lifang He, Lifu Huang, Michael Backes, Neil Zhenqiang Gong, Philip S. Yu, Pin-Yu Chen, Quanquan Gu, Ran Xu, Rex Ying, Shuiwang Ji, Suman Jana, Tianlong Chen, Tianming Liu, Tianyi Zhou, William Wang, Xiang Li, Xiangliang Zhang, Xiao Wang, Xing Xie, Xun Chen, Xuyu Wang, Yan Liu, Yanfang Ye, Yinzhi Cao, and Yue Zhao. 2024. TrustLLM: Trustworthiness in Large Language Models. *CoRR* abs/2401.05561 (2024). *arXiv:2401.05561*
- [65] Pang-Ning Tan, Michael S. Steinbach, and Vipin Kumar. 2005. *Introduction to Data Mining*. Addison-Wesley.
- [66] Yanchao Tan, Zihao Zhou, Hang Lv, Weiming Liu, and Carl Yang. 2023. WalkLM: A Uniform Language Model Fine-tuning Framework for Attributed Graph Embedding. In *Advances in Neural Information Processing Systems 36: Annual Conference on Neural Information Processing Systems*.
- [67] Hugo Touvron, Louis Martin, Kevin Stone, Peter Albert, Amjad Almahairi, Yasmine Babaei, Nikolay Bashlykov, Soumya Batra, Prajjwal Bhargava, and et al. 2023. Llama 2: Open Foundation and Fine-Tuned Chat Models. *CoRR* abs/2307.09288 (2023). *arXiv:2307.09288*
- [68] Petar Veličković, Guillem Cucurull, Arantxa Casanova, Adriana Romero, Pietro Lio, and Yoshua Bengio. 2017. Graph attention networks. *arXiv preprint arXiv:1710.10903* (2017).
- [69] Haixun Wang and Charu C Aggarwal. 2010. A survey of algorithms for keyword search on graph data. *Managing and mining graph data* (2010), 249–273.
- [70] Xiao Wang, Deyu Bo, Chuan Shi, Shaohua Fan, Yanfang Ye, and Philip S. Yu. 2023. A Survey on Heterogeneous Graph Embedding: Methods, Techniques, Applications and Sources. *IEEE Trans. Big Data* 9, 2 (2023), 415–436.
- [71] Yujie Wang, Hu Zhang, Jiye Liang, and Ru Li. 2023. Dynamic Heterogeneous-Graph Reasoning with Language Models and Knowledge Representation Learning for Commonsense Question Answering. In *Proceedings of the 61st Annual Meeting of the Association for Computational Linguistics*. Association for Computational Linguistics, 14048–14063.
- [72] Richard J Whitley. 2002. Herpes simplex virus infection. In *Seminars in pediatric infectious diseases*, Vol. 13. Elsevier, 6–11.
- [73] Zonghan Wu, Shirui Pan, Fengwen Chen, Guodong Long, Chengqi Zhang, and Philip S. Yu. 2021. A Comprehensive Survey on Graph Neural Networks. *IEEE Trans. Neural Networks Learn. Syst.* 32, 1 (2021), 4–24.
- [74] Zhenqin Wu, Bharath Ramsundar, Evan N Feinberg, Joseph Gomes, Caleb Geniesse, Aneesh S Pappu, Karl Leswing, and Vijay Pande. 2018. MoleculeNet: a benchmark for molecular machine learning. *Chemical science* 9, 2 (2018), 513–530.
- [75] YQ Xia, KN Zhao, AD Zhao, JZ Zhu, HF Hong, YL Wang, and SH Li. 2019. Associations of maternal upper respiratory tract infection/influenza during early pregnancy with congenital heart disease in offspring: evidence from a case-control study and meta-analysis. *BMC Cardiovascular Disorders* 19 (2019), 1–13.
- [76] Yasin Abbasi Yadkori, Ilja Kuzborskij, András György, and Csaba Szepesvári. 2024. To Believe or Not to Believe Your LLM. *arXiv preprint arXiv:2406.02543* (2024).
- [77] Carl Yang, Yuxin Xiao, Yu Zhang, Yizhou Sun, and Jiawei Han. 2022. Heterogeneous Network Representation Learning: A Unified Framework With Survey and Benchmark. *IEEE Trans. Knowl. Data Eng.* 34, 10 (2022), 4854–4873.
- [78] Jianye Yang, Wu Yao, and Wenjie Zhang. 2021. Keyword Search on Large Graphs: A Survey. *Data Sci. Eng.* 6, 2 (2021), 142–162.
- [79] Yuning You, Tianlong Chen, Yongduo Sui, Ting Chen, Zhangyang Wang, and Yang Shen. 2020. Graph contrastive learning with augmentations. *Advances in Neural Information Processing Systems* 33 (2020), 5812–5823.
- [80] Biao Zhang, Barry Haddow, and Alexandra Birch. 2023. Prompting large language model for machine translation: A case study. In *International Conference on Machine Learning*. PMLR, 41092–41110.
- [81] Muhan Zhang, Pan Li, Yinglong Xia, Kai Wang, and Long Jin. 2021. Labeling trick: A theory of using graph neural networks for multi-node representation learning. *Advances in Neural Information Processing Systems* 34 (2021), 9061–9073.
- [82] Zhilu Zhang and Mert Sabuncu. 2018. Generalized cross entropy loss for training deep neural networks with noisy labels. *Advances in Neural Information Processing Systems* 31 (2018).
- [83] Jianan Zhao, Meng Qu, Chaozhao Li, Hao Yan, Qian Liu, Rui Li, Xing Xie, and Jian Tang. 2022. Learning on Large-scale Text-attributed Graphs via Variational Inference. In *The Eleventh International Conference on Learning Representations*.
- [84] Jie Zhou, Ganqu Cui, Shengding Hu, Zhengyan Zhang, Cheng Yang, Zhiyuan Liu, Lifeng Wang, Changcheng Li, and Maosong Sun. 2020. Graph neural networks: A review of methods and applications. *AI Open* 1 (2020), 57–81.
- [85] Yanqiao Zhu, Yichen Xu, Feng Yu, Qiang Liu, Shu Wu, and Liang Wang. 2020. Deep graph contrastive representation learning. *arXiv preprint arXiv:2006.04131* (2020).
- [86] Yanqiao Zhu, Yichen Xu, Feng Yu, Qiang Liu, Shu Wu, and Liang Wang. 2021. Graph contrastive learning with adaptive augmentation. In *Proceedings of the web conference 2021*. 2069–2080.
- [87] Yuchen Zhuang, Yue Yu, Kuan Wang, Haotian Sun, and Chao Zhang. 2024. Toolqa: A dataset for llm question answering with external tools. *Advances in Neural Information Processing Systems* 36 (2024).

A APPENDIX

A.1 Details of Path Textualization

For homogeneous text-attributed graphs, for example, in citation network, where edges represent citation relationships and node text attributes are titles, abstracts, etc:

Path textualization for homogeneous graphs.

Path: $P = (v_1, v_2, v_3)$

Text attributes:

\mathcal{X}_{v_1} : { Title: forecasting the cost of processing multi join queries ... Abstract:...};

\mathcal{X}_{v_2} : { Title: challenges of integrating a priori information efficiently... Abstract:...};

\mathcal{X}_{v_3} : { Title: n optimal geographical caching ... Abstract:...}

$\Phi(\cdot)$ with template: <the paper with content \mathcal{X}_{v_1} cites the paper with content \mathcal{X}_{v_2} cites the paper with content \mathcal{X}_{v_3} >

Output: <the paper with content "forecasting the cost of processing multi join queries..." cites the paper with content "integrating a priori information efficiently..." cites the paper with content "n optimal geographical caching...">

For heterogeneous text-attributed graphs, for example, in PubMed, where nodes have four types: gene, disease, chemical, and species, and edges have multiple meanings:

Path textualization for heterogeneous graphs.

Path: $P = (v_1, v_2, v_3)$

Text attributes: \mathcal{X}_{v_1} : CREBBP $\mathcal{X}_{e_{1,2}}$: causing \mathcal{X}_{v_2} : SIV-infected $\mathcal{X}_{e_{2,3}}$: and \mathcal{X}_{v_3} : respiratory chain deficiency

$\Phi(\cdot)$: < $\mathcal{X}_{v_1} | \mathcal{X}_{e_{1,2}} | \mathcal{X}_{v_2} | \mathcal{X}_{e_{2,3}} | \mathcal{X}_{v_3}$ >

Output: < CREBBP causing SIV-infected and respiratory chain deficiency >

A.2 Proof of Lemma 4.1

PROOF. Based on the chain rule of conditional probability [9], we can derive the probability of Path-LLM predicting the L2SP-based text T as:

$$\prod_{i=1}^{\ell} \prod_{j=j^*}^{\tilde{j}} p(t_j^{v_i} | t_{<j}^{v_{<i}}) = \prod_{i=1}^{\ell} p(\{t_{j^* \leq j \leq \tilde{j}}^{v_i}\} | t_{<j^*}^{v_{<i}}) \quad (4)$$

Due to $\Phi(\mathcal{X}_{v_i}) = \{t_{j^* \leq j \leq \tilde{j}}^{v_i}\}$ and $\Phi(\mathcal{X}_{v_{<i}}) = t_{<j^*}^{v_{<i}}$, we can know that:

$$\prod_{i=1}^{\ell} p(\{t_{j^* \leq j \leq \tilde{j}}^{v_i}\} | t_{<j^*}^{v_{<i}}) = \prod_{i=1}^{\ell} p(\Phi(\mathcal{X}_{v_i}) | \Phi(\mathcal{X}_{v_{<i}})) \quad (5)$$

$\Phi(\mathcal{X}_{v_{<i}})$ denotes $\Phi(\mathcal{X}_v)$ satisfying the condition of the node index being less than i . Obviously, $\prod_{i=1}^{\ell} p(\Phi(\mathcal{X}_{v_i}) | \Phi(\mathcal{X}_{v_{<i}}))$ is similar to $\prod_{i=1}^{\ell} p(\mathcal{X}_{v_i} | \mathcal{X}_{v_{<i}})$. Thus, we can obtain that:

$$\prod_{i=1}^{\ell} \prod_{j=j^*}^{\tilde{j}} p(t_j^{v_i} | t_{<j}^{v_{<i}}) \approx \prod_{i=1}^{\ell} p(\mathcal{X}_{v_i} | \mathcal{X}_{v_{<i}}) \quad (6)$$

Proved. Thus, during Path-LLM pre-training, L2SP-based texts generation can be regarded as the L2SP generation. \square

A.3 Experiment Settings

For node classification, the MLP training epoch is set to 50, compared to 2000 epochs in WalkLM. For link prediction, the MLP training epoch is set to 100 without any additional models. Compared to adding LMNN trained for 1000 epochs and MLP trained for 1000 epochs in WalkLM. Noisy graph embeddings can improve after training with thousands of MLP iterations and additional model stacking. Thus, the high-quality and more robust graph embeddings cannot be revealed in WalkLM's setting.

Table 5: Appendix experimental results on Citeseer.

Datasets	Citeseer			
	Node classification		Link prediction	
Tasks	Macro-F1	Micro-F1	AUC	Accuracy
GCN	0.4627	0.4900	0.6392	0.6052
GraphSage	0.4903	0.5240	0.7822	0.5227
GATv2	0.4816	0.5530	0.7488	0.5986
WalkLM	0.5761	0.6616	0.9149	0.8424
Llama 2	0.6739	0.7281	0.9290	0.8550
Path-LLM (Ours)	0.6818	0.7363	0.9385	0.8671

Table 6: Appendix experimental results on ARXIV.

Datasets	ARXIV			
	Node classification		Link prediction	
Tasks	Macro-F1	Micro-F1	AUC	Accuracy
GCN	0.1681	0.5199	0.5216	0.4415
GraphSage	0.1962	0.5581	0.5110	0.3120
GATv2	0.1199	0.4443	0.2550	0.6120
WalkLM	0.3337	0.5751	0.8799	0.7923
Llama 2	0.4123	0.5948	0.9157	0.8379
Path-LLM (Ours)	0.4226	0.6091	0.9333	0.8579

Table 7: Ablation study of node classification.

Datasets	AXIV		Citeseer	
	Macro-F1	Micro-F1	Macro-F1	Micro-F1
LLM	0.4123	0.5948	0.6739	0.7281
LLM + 1hop	0.4164	0.6069	0.6770	0.7250
LLM + RW	0.4149	0.6060	0.6701	0.7288
LLM + Random short	0.4187	0.6071	0.6742	0.7269
LLM + Long SP	0.4149	0.6039	0.6702	0.7275
LLM + L2SP	0.4226	0.6091	0.6818	0.7363

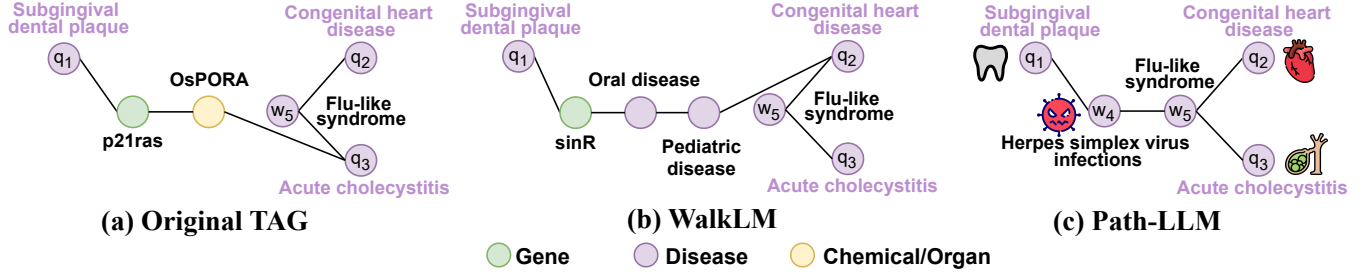


Figure 8: Case study in keyword search. Here, three keywords are $Q = \{q_1: \text{subgingival dental plaque}, q_2: \text{congenital heart disease}, q_3: \text{acute cholecystitis}\}$. We show the Steiner trees returned by uniform weight, WalkLM-based weight, and Path-LLM-based weight.

Table 8: Ablation study of link prediction.

Datasets	AXIV		Citeseer	
Metrics	AUC	Accuracy	AUC	Accuracy
LLM	0.9157	0.8379	0.9290	0.8550
LLM + 1hop	0.9247	0.8455	0.9331	0.8594
LLM + RW	0.9255	0.8478	0.9334	0.8546
LLM + Random Short	0.9238	0.8410	0.9338	0.8673
LLM + Long SP	0.9287	0.8497	0.9301	0.8577
LLM + L2SP	0.9333	0.8579	0.9385	0.8671

Table 9: Ablation study of L2SP and long shortest path on Citeseer.

Datasets	Citeseer			
Tasks	Node classification		Link prediction	
Metrics	Macro-F1	Micro-F1	AUC	Accuracy
long num1	0.6709	0.7272	0.9219	0.8505
L2SP num1	0.6809	0.7338	0.9305	0.8608
long num5	0.6678	0.7263	0.9305	0.8570
L2SP num5	0.6773	0.7332	0.9343	0.8641
long num10	0.6702	0.7275	0.9301	0.8577
L2SP num10	0.6776	0.7332	0.9316	0.8662

A.4 Experiment Results on Citeseer and ARXIV

As shown in Table 5 and Table 6, for node classification, Path-LLM shows an average performance gain of 16.27% on ARXIV and 14.82% on Citeseer, further demonstrating its superiority. For link prediction, on citation networks, particularly the Citeseer dataset, Path-LLM performance has less increase, which is an average 1.22% gain of pure LLM, due to the richness of semantic information, resulting in less impact on the structure.

A.5 Ablation Studies

Table 7 and Table 8 show the results of our proposed L2SP compared to other path structures.

Long-to-short shortest paths outperform long shortest paths. Table 9 show that long-to-short shortest paths perform better than long shortest paths, whether on a citation network or a

Table 10: Less words experiment on Citeseer. (words num 5)

Datasets	Citeseer			
Tasks	Node classification		Link prediction	
Metrics	Macro-F1	Micro-F1	AUC	Accuracy
LLM	0.5456	0.6064	0.8111	0.7375
LLM + 1hop	0.5594	0.6195	0.8244	0.7457
LLM + RW	0.5520	0.6104	0.8166	0.7277
LLM + Random Short	0.5632	0.6264	0.8278	0.7473
LLM + Long SP	0.5480	0.6161	0.8215	0.7457
LLM + L2SP	0.5687	0.6274	0.8414	0.7568

biomedical network. However, the effect is more pronounced on a text-sparse graph.

L2SP’s structural advantage is more pronounced in graphs with fewer text attributes. To validate that the path structure has a more significant impact on Path-LLM in a text-sparse graph than in a text-rich graph, we disrupt the semantic information in the text-rich graph. We only use five words as each node’s text attribute to explore whether the performance gap between different path structures will grow. Path-LLM’s performance is more significant after disrupting the semantic information in the text-rich graph, as shown in Table 10. Our proposed shortest path structure is superior to random walk, 1-hop neighbors, and long shortest paths.

A.6 Case Study

Figure 8 shows Steiner trees based on three given keywords that are not directly related $\{q_1: \text{subgingival dental plaque}, q_2: \text{congenital heart disease}, q_3: \text{acute cholecystitis}\}$. From the graph structure perspective, the Path-LLM-based weights demonstrate superior characteristics, featuring fewer edges and establishing a more robust correlation among the three keywords. From a graph semantics perspective, the subtree indicated by Path-LLM suggests intriguing potential correlations. For instance, patients with periodontal disease carrying (q_1) subgingival dental plaque will test positive for (w_4) herpes simplex virus [2, 31, 62]. Patients infected with (w_4) the herpes simplex virus also exhibit (w_5) influenza symptoms such as fever, chills, and body aches [6, 72]. Similarly, patients with (q_4) acute cholecystitis also display (w_5) influenza symptoms [16, 21]. Notably, maternal (w_5) influenza symptoms lead to an elevated risk of newborn babies with (q_3) congenital heart disease [40, 49, 54, 75], emphasizing the need for further investigation.